Scalable Computing: Practice and Experience, ISSN 1895-1767, http://www.scpe.org
© 2024 SCPE. Volume 25, Issues 6, pp. 4898–4912, DOI 10.12694/scpe.v25i6.3403

MPC OPTIMIZATION ALGORITHM AND STRATEGY FOR HVAC SYSTEM UNDER SMART CITY CONSTRUCTION

LEI WANG*

Abstract. As a giant in energy consumption, buildings urgently need to optimize control strategies for the main energy consuming equipment inside buildings. It is of great significance to design advanced control algorithms to improve the efficiency of the main energy consuming equipment in buildings, namely air conditioning, in the current energy shortage. The model predictive control algorithms and strategies were used in this study to control the HVAC system to improve the energy utilization of the city. Then linear matrix inequality with robust model predictive feedback controller was used to optimize and get the model predictive control optimization algorithm. The research results showed that, under the influence of different factors, the three regions controlled by the model predictive control optimization algorithm showed a little overshooting in the initial state. But it was quickly corrected after adjustment. Meanwhile, the average tracking error of temperature and humidity in each region was 0.139℃ and 0.13g/kg dry air, respectively. The average predicted mean vote was 0.32. In actual office buildings, the proposed algorithm controlled the temperature within the reference value range of 0.1℃ throughout the entire process. The total electricity consumption and electricity price costs were reduced by 12.11% and 22.54%, respectively. In summary, the proposed method has good performance for HVAC system application, which can effectively realize energy saving and emission reduction and improve human comfort. This method makes important contributions to promote the construction of smart cities and the development of green buildings.

Key words: Smart city; HVAC system; MPC optimization algorithm; Control strategy; Energy efficiency

1. Introduction. In recent years, it is important to realize the dual-carbon target. Green buildings need to take up the heavy responsibility of energy saving and emission reduction work, and green and sustainable economic development needs to be realized [1-2]. At the same time, the carbon emissions of the construction industry account for over 50% of the total national energy consumption, while Heating, Ventilation and Air Conditioning (HVAC) systems account for about 60% of the total building energy consumption. Therefore, energy efficiency can be reduced by optimizing and controlling the HVAC system in buildings [3-4]. In addition, people spend more than 80% of their daily lives in buildings. If the HVAC system reduces human comfort due to energy saving, it can be a serious obstacle to learning efficiency and work [5]. At present, the traditional algorithms used in HVAC systems include Programmable Logic Controller (PLC) and Proportional Integration Differentiation (PID). The former has advantages such as simple operation and easy maintenance. But PLC lacks sufficient computing and analysis capabilities in practical applications and is difficult to coordinate the contradiction between human comfort and energy conservation. The latter is prone to the contradiction between speed and overshoot in closed-loop systems, and the inhibitory ability of the integration link is not significant for time-varying disturbances. Model Predictive Control (MPC), as a mainstream emerging control algorithm in recent years, can fully consider the multivariate constraints of the system and predict the future dynamics of the system to maximize the desired performance and achieve stable control of the system [6-7]. Moreover, the MPC algorithm can take into account multiple input factors, such as indoor and environmental temperature, indoor and external airflow, power costs, etc. Meanwhile, MPC can effectively balance the contradiction between energy consumption and indoor comfort to achieve optimal results. Due to deficiencies in the modeling of HVAC systems, the operating environment of HVAC systems is variable based on the comfort control. At the same time, the indoor temperature and humidity model is time-varying, which cannot avoid deviations from the actual system during the control process. From the perspective of energy-saving control, the instantaneous energy consumption dynamic model of HVAC is affected by controllable refrigeration or heating loads and uncontrollable lighting and electrical loads. Meanwhile, there are nonlinear parts in the model, which pose

*Sichuan College of Architectural Technology, Deyang 618000, Sichuan, China (leiwangl@outlook.com)

great difficulty to the design of MOC controllers. The study designed the MPC algorithm for multi-zone HVAC room control to solve the contradiction between comfort and energy saving in HVAC. Then the MPC algorithm was optimized based on Linear Matrix Inequality (LMI) to obtain the MPC Optimization Algorithm (MPC-O). The research aims to optimize the comfort of the indoor environment while enabling the HVAC system to ensure continuous low-energy operation. Meanwhile, this paper aims to enhance the intelligent level and sustainable development of urban construction. There are two main innovations in the study. One is the introduction of the MPC and MPC-O algorithms to control the HVAC system, and the other is the simultaneous realization of the comfort and energy saving in the indoor environment. The research structure is mainly divided into four parts. The first part is a review of relevant research results. In the second part, first, the control principle of MPC algorithm in HVAC systems is introduced, then a multi-zone HVAC room control based on MPC algorithm and strategy is proposed, and finally MPC-O strategy control is designed for the indoor thermal comfort. The third part is the performance analysis of the MPC algorithm in multi-zone HVAC room control and the effectiveness analysis of the HVAC system using the MPC-O control strategy in Wuxi summer. The last part is a summary of the research.

2. Related works. With the continuous promotion of smart city construction, the HVAC system becomes the main source of building energy consumption. The traditional HVAC system has difficulty to meeting the requirements of green buildings for comfort and energy saving. Numerous scholars have discussed this in depth. Li proposed a load estimation method for HVAC systems in large public stadiums and analyzed the influencing factors of HVAC air conditioning. Experiments showed that the method was robust, had good adaptability to the model parameters, and had a good fit between the load estimation results and the actual values. The maximum running time was less than 12.8s, which had a good performance in practical applications [8]. Satar et al. investigated the existence of noise and vibration problems in HVAC systems when a car was heating up and developed a laboratory scale model of the HVAC system. The results showed that noise was heard in the operating frequency range of 200-300 Hz, and that the generation of noise and vibration was more intense when the HVAC system was running [9] Jani explored the effect of desiccant-assisted HVAC air-conditioning for the building environments and discussed the need for a more energy efficient and environmentally friendly desiccant to replace traditional HVAC systems based on vapor compression [10]. Vogt M et al. designed a special sized HVAC system to operate a dry room to provide a safe and well conditioned environment during battery assembly. A validated simulation model of the HVAC system was used to investigate the virtual deployment of the system in five different locations around the world. Deployed in five different locations around the world and operated for one year, the study showed that the system was able to provide an accurate economic and environmental assessment of each location [11].

The MPC algorithm is a new type of control algorithm, which adopts control strategies such as multi-step prediction, rolling optimization, and error correction. The MPC algorithm has better robustness and control effect and has advantages in dealing with high-order, multi-constraint, and nonlinear system problems. The classical control method PID has poor control effect in real engineering because it is difficult to deal with nonlinear, multi-constraint, uncertain, and time-varying control systems. Wang Z et al. design a path optimization algorithm based on improved A* for the path planning of a hexapod robot, and a MPC-based motion tracking controller was used for path tracking. This method was used to solve the traditional path planning problem. The experimental results verified the performance of the method, which solved the problems of security, too many turns, and insufficient smoothing that existed in the traditional path planning method [12]. Ren J et al. found that MPC was less used in missile guidance law, so they deduced an explicit linear discrete time model as a prediction model, and a fast algorithm was given for the MPC guidance law. The simulation results showed that the MPC guidance law met the real-time requirements well [13]. He N et al. developed an algorithm to solve the perturbation nonlinear problem of MPC. Meanwhile, the error gradient and cumulative event-driven MPC framework was designed. The research results showed that this method effectively reduced the computational burden of the MPC controller and verified its feasibility and stability [14]. Wang S et al. proposed an adaptive wind power MPC-O based on the problem that the existing MPC strategy could not reflect the stochastic fluctuation of wind power. The experimental results verified the robustness, stability, and grid security of this method [15].

Based on the above content, the current research on HVAC systems and MPC algorithms focuses on

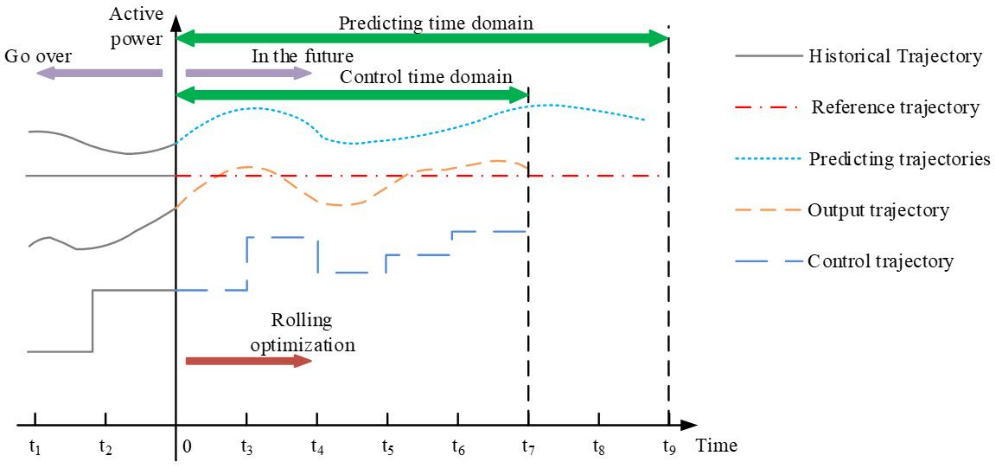

Fig. 3.1: Schematic diagram of the basic principle of MPC algorithm

addressing building thermal dynamic characteristics through measures taken in the control process. The MPC algorithm is optimized to minimize external uncertain disturbance factors and improve human comfort is currently a research focus. Therefore, the contradiction between human comfort and energy conservation can be addressed, and the functional pressure can be alleviated during peak hours on the power grid. Based on multi-zone HVAC rooms, a MPC-O algorithm based on LMI and robust model predictive feedback controller is proposed to directly control the efficiency of HVAC compressors, achieving both energy cost savings and ensuring indoor human comfort.

3. The MPC-O algorithm and policy control for HVAC systems. The HVAC system, as the core part of building environment control, is widely used in commercial facilities and other buildings. But this system has problems such as high energy consumption and difficulty in meeting human comfort needs. Aiming at the above problems, the study firstly explores the control principle of MPC algorithm in the HVAC system. Then the MPC algorithm and strategy are designed for control under multi-zone HVAC room. Finally, the MPC-O algorithm and control strategy are proposed for the internal comfort of indoor environment.

3.1. The MPC algorithm for control in the HVAC system. The MPC algorithm belongs to an advanced process control method, which is widely used in various fields. This system is applicable to linear and nonlinear systems, which can consider various constraints of spatial state variables. However, the mainstream PID control algorithms only consider the various constraints of the input and output variables [16-18]. The MPC algorithm mainly has the following three basic principles. The first is a predictive model, mainly based on the object's cubic information and future inputs, predicting the future output of the system. The second is rolling optimization, which is different from the traditional optimal control of the fundamental point through the optimal value of a certain performance indicator to determine the role of the control [19-20]. Finally, the prediction results are corrected by detecting the actual output of the object at the new sampling moment. At the same time, the real-time information is utilized to avoid the deviation of the control from the ideal state caused by the model mismatch or environmental disturbances. The basic principles of the MPC algorithm are illustrated in Fig. 3.1.

In Fig. 3.1, the MPC algorithm is able to solve the optimization problem for a local prediction range at each control moment and make corrections by predicting the future conditions continuously rolling forward. However, the application of the MPC algorithm in the HVAC systems has the following problems. They include the uncertainty of the external environment affects more factors and the existence of the nonlinear part of the model may have an impact on the MPC control strategy during the modeling. Therefore, the MPC algorithm needs to be improved. In the HVAC system, there are two typical control methods, namely, variable air volume

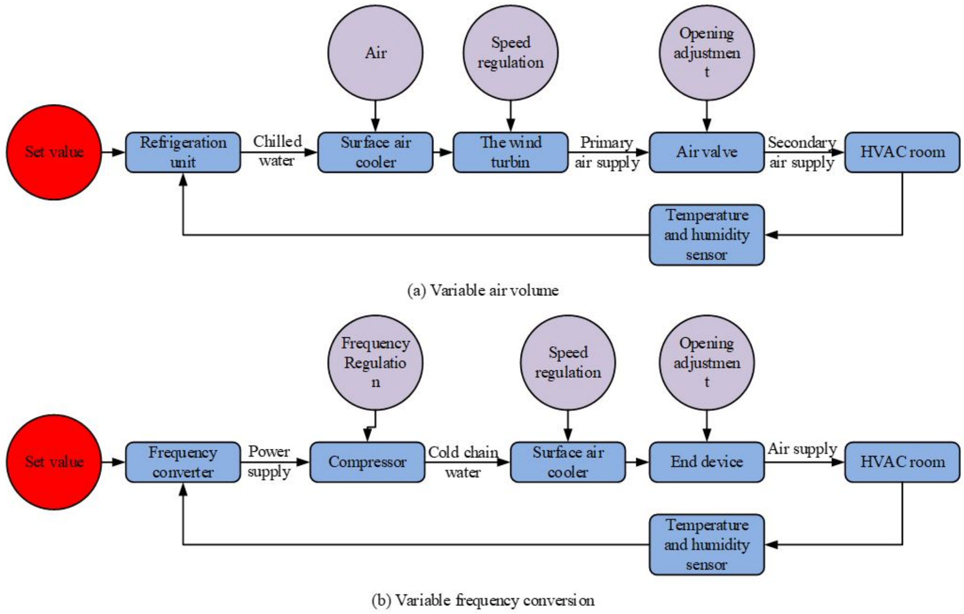

Fig. 3.2: Principles of variable air volume and variable frequency control in HVAC systems

and variable frequency, and the specific control principles are shown in Fig. 3.2.

Figures 3.2 (a) and 3.2 (b) show the HVAC system variable air volume and variable frequency corresponding to the principle of control. Variable air volume directly controls the air volume of the outlet. The smaller fan capacity and different indoor comfort requirements have a strong flexibility. In addition, the air conditioning end equipment is the most important influence on the variable air volume HVAC system. The state can quickly respond to changes in the indoor environment. The development of this system also has greater prospects for comfort. The principle of variable frequency control is to increase the frequency converter to control the compressor frequency. Therefore, the cooling rate can be adjusted and the energy-saving effect is obvious, which can maintain indoor human comfort around the clock and easy to access the smart grid. The study designs the control strategy of HVAC system based on the MPC algorithm for the comfort and energy saving control.

3.2. Multi-zone HVAC room control based on MPC algorithms and strategies. Since most studies consider the interior of the room in which the HVAC system is located as a whole and ignore the losses generated by air flow, environmental differences, etc., the final results of the algorithm can only achieve the theoretical optimum. Therefore, the study uses hydrodynamic computational methods to construct a thermodynamic model of a multi-zone HVAC room. At the same time, an MPC control strategy that can be optimized with multiple objectives is designed. The multi-zone HVAC room modeling process is as follows. Firstly, the following assumptions are made. The room is divided into air supply area (area A), air return area (area B), and working area (area C). Each area is represented by a state. The surface temperature of the inner and outer walls of the room is represented by a set of total values. Only the light bulb is a heat source in the air supply area and there is no source of moisture. There is no heat source and moisture source in the air return area. All the heat sources in the working area are heat and moisture sources. All the heat sources in the working area are heat and moisture sources. There are no heat and moisture sources in the return air zone. All heat sources in the work zone have fixed surface temperatures. The convective heat transfer coefficient between adjacent spaces and walls or heat sources is fixed. The temperature measurement data come from thermistors, and the humidity measurement data come from resistive sensors. Under the control of the variable air volume HVAC system, the mass-energy conservation law leads to the temperature and humidity model of area A, which is shown in equation (3.1).

$$\begin{cases} \rho_a V_{a,A} \frac{dh_{a,A}}{dt} = AP_{a,i}\left(h_{a,i} - h_{a,A}\right) + \Delta q_{a,A} \\ \rho_a V_{a,A} \frac{dW_{a,A}}{dt} = AP_{a,i}\left(W_{a,i} - W_{a,A}\right) \\ C_{iw,A}\rho_{iw} V_{iw,A} \frac{dT_{iw,A}}{dt} = \vartheta_{iw,A} K_{iw,A}\left(T_{a,A} - T_{iw,A}\right) \end{cases} \tag{3.1}$$

In equation (3.1), ρ_a and ρ_{iw} are the densities of the air corresponding to the inner wall. $AP_{a,i}$, $h_{a,i}$, and $W_{a,i}$ are the flow rate, enthalpy, and humidity of the air supplied from the air outlet. $h_{a,A}$, $h_{a,A}$, $W_{a,A}$, and $T_{a,A}$ are the volume, enthalpy, humidity, and temperature of the air in region A, respectively. $C_{iw,A}$, $V_{iw,A}$, $K_{iw,A}$, $\vartheta_{iw,A}$, and$T_{iw,A}$ are the specific heat capacity, volume, area, convective heat transfer coefficient, and temperature of the air between the region A and the inner wall, respectively. $\Delta q_{a,A}$ denotes the thermal growth rate of air in region A. The temperature and humidity model of region B is shown in equation (3.2). The temperature and humidity models in the region B are expressed by equation (3.2).

$$\begin{cases} \rho_a V_{a,B} \frac{dh_{a,B}}{dt} = AP_{a,i}\left(h_{a,i} - h_{a,B}\right) + \Delta q_{a,B} \\ \rho_a V_{a,B} \frac{dW_{a,B}}{dt} = AP_{a,i}\left(W_{a,i} - W_{a,B}\right) \\ C_{iw,B}\rho_{iw} V_{iw,B} \frac{dT_{iw,B}}{dt} = \vartheta_{iw,B} K_{iw,B}\left(T_{a,B} - T_{iw,B}\right) \end{cases} \tag{3.2}$$

In equation (3.2), $V_{a,B}$, $h_{a,B}$, $W_{a,B}$, and$T_{a,B}$ are the volume, enthalpy, humidity, and temperature of region B, respectively. $\Delta q_{a,B}$ represents the thermal growth rate of the air in region B. $C_{iw,B}$, $V_{iw,B}$, $K_{iw,B}$, $\vartheta_{iw,B}$, and$T_{iw,B}$ are the specific heat capacity, volume, area of the region, convective heat transfer coefficient, and temperature of the air between region B and the inner wall, respectively. The temperature and humidity of region C are modeled as in equation (3.3).

$$\begin{cases} \rho_a V_{a,C} \frac{dh_{a,C}}{dt} = AP_{a,i}\left(h_{a,A} - h_{a,C}\right) + \Delta q_{a,C} \\ \rho_a V_{a,C} \frac{dW_{a,C}}{dt} = AP_{a,i}\left(W_{a,A} - W_{a,C}\right) + \Delta e_{a,C} \\ C_{iw,C}\rho_{iw} V_{iw,C} \frac{dT_{iw,C}}{dt} = \vartheta_{iw,C} K_{iw,C}\left(T_{a,C} - T_{iw,C}\right) \\ C_{ew,C}\rho_{ew} V_{ew,C} \frac{dT_{ew,C}}{dt} = \vartheta_{ew,C} K_{ew,C}\left(T_{a,C} - T_{ew,C}\right) + \frac{\beta_{ew} K_{ew,C}}{ts_{ew}}\left(T_{ew,e} - T_{ew,C}\right) \end{cases} \tag{3.3}$$

In equation (3.3), ρ_{ew}, β_{ew}, andts_{ew} are the density, thermal conductivity, and thickness of the exterior wall, respectively. $V_{a,C}$, $h_{a,C}$, $W_{a,C}$, $T_{a,C}$, $\Delta q_{a,C}$, and $\Delta e_{a,C}$ are the volume, enthalpy, humidity, temperature, thermal growth rate, and humidity growth rate of the air in Area C, respectively. At typical indoor temperature, the enthalpy of human exhaled gas h_o is related to the temperature $T_{h,o}$ and humidity $W_{h,o}$, and the expression is shown in equation (3.4).

$$\begin{cases} T_{h,o} = 0.066T_{a,C} + 32.6 \\ W_{h,o} = 0.2W_{a,C} + 0.029 \end{cases} \tag{3.4}$$

In equation (3.4), human lung ventilation rate G_{is} and body surface area $A_{ew,c}$ are calculated in equation (3.5).

$$\begin{cases} G_{is} = 1.43 \bullet 10^{-6} E A_{ew,c} \\ A_{ew,c} = 0.202 m^{0.425} H^{0.725} \end{cases} \tag{3.5}$$

In equation (3.5), E, m, and$H$ represent the metabolic rate, weight, and height of indoor members, respectively. The surface temperature of the exterior wall $T_{ew,a}$ is expressed in equation (3.6).

$$T_{ew,a} = T_{a,o} + \frac{\delta S}{\alpha_{ew,a}} \tag{3.6}$$

In equation (3.6), $T_{a,o}$ represents the temperature of the external environment. $\alpha_{ew,a}$ represents the convective heat exchange coefficient between the external wall and the air of the external environment. δ and S are the absorption coefficient and intensity of the solar radiation, respectively. The enthalpy of air h_a is calculated as equation (3.7).

$$h_a = C_a T_a + 2.5 \bullet 10^6 \bullet W_a \tag{3.7}$$

In equation (3.7), C_a, T_a, and W_a are the specific heat capacity, temperature, and humidity of air, respectively. The above model needs to be transformed into a state-space model to facilitate the MPC algorithm to control the temperature and humidity of different regions, and the transformed expression is shown in equation (3.8).

$$\begin{cases} \chi \dot{x} = D_q \chi x + L_q \chi u \\ y = Q\left(\chi x + x_0\right) \\ \chi x = \left[\chi T_{a,A} \chi W_{a,A} \chi T_{iw,A} \chi T_{a,B} \chi W_{a,B} \chi T_{iw,B} \chi T_{a,C} \chi W_{a,C} \chi T_{iw,C} \chi T_{ew,C}\right]^T \\ \chi u = \left[\chi T_{a,i} \chi W_{a,i} \chi AP_{a,i} \chi T_{a,o} \chi S\right]^T \end{cases} \tag{3.8}$$

In equation (3.8), D_q, L_q, and Q are the state matrix, control matrix and output matrix, respectively. χx and χu are the state variables and input variables respectively. x_0 represents the steady state point. Finally, the inputs are the air supply volume and the air supply temperature and humidity, and the outputs are the temperature and humidity of the three regions. The above linear state space model can not be directly used in the MPC strategy, which needs to be discretized. The discrete-time state space model after processing, that is, the prediction model is expressed by equation (3.9).

$$\begin{cases} \chi x\left(k+1\right) = D_d \chi x\left(k\right) + L_d \chi u\left(k\right) \\ y\left(k\right) = Q\left(\chi x\left(k\right) + x_0\right) \\ D_d = e^{D_Q T_s} \\ L_d = \left(\int_0^{T_s} e^{D_Q T} dt\right) L_q \end{cases} \tag{3.9}$$

In equation (3.9), k and T_s are the sampling time and interval, respectively. D_d and L_d are the state matrix and input matrix of the system, respectively. The study designs the performance index function with multiple optimization objectives to ensure the comfort state in the room, and the calculation is shown in equation (3.10).

$$\begin{cases} J_{\min U} = \left(Y - R\right)^T \tilde{O}\left(Y - R\right) + U^T \tilde{R} U \\ O = diag\left[10^4, 10^4, 10^5, 10^4, 10^5, 10^4,\right] \\ R = \omega \bullet diag\left[50, 50, 5, 1, 1\right] \end{cases} \tag{3.10}$$

In equation (3.10), O and R are the weights of the tracking error and control inputs, respectively. ω represents reducing the coefficient of the control weight matrix. Through the above operations, the MPC strategy focuses more on the tracking of temperature and humidity in the room and copes with frequent changes in reference values. At this point the ζ function has been converted to a standard quadratic programming problem. Finally, the MPC algorithm is able to explicitly process various equations and inequality constraints. The input air supply is determined by the fan speed and the valve opening of the terminal equipment, in addition to considering the rate of change of the input. As a result, a multi-zone HVAC room flow based on MPC strategy control under variable air volume control is constructed, as shown in Fig. 3.3.

In Fig. 3.3, the optimized quantities are solved according to the constructed objective function related to temperature and humidity and air supply quantity. Finally, the actual state quantities corresponding to different regions are obtained, and the above process is looped until the end of the simulation.

3.3. Improved indoor comfort based on the MPC-O strategy control. The single-zone indoor model gives more uncertain external factors compared with the multi-zone HVAC room temperature and humidity model. Because there is the euclidean interaction of heat transfer coefficients between different zones and the influence of the outdoor climate. This results in a more difficult process to describe the thermal dynamics in the environment. Therefore, the study uses LMI with robust model predictive feedback controller to improve it and obtain the MPC-O strategy. LMI is a method for matrix inequality constrained optimization

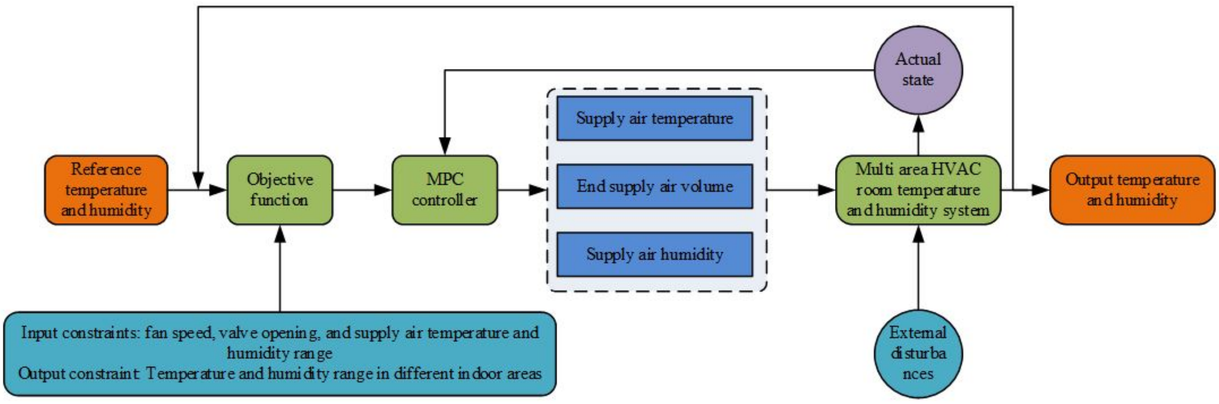

Fig. 3.3: Multi-zone HVAC room process control based on MPC strategy under variable air volume control

problems, commonly used in the design and analysis of control systems. The cores are to describe the constraints of the system through linear matrix inequalities and to improve the performance and stability by solving matrix inequality optimization problems. The study expresses the covariates using the multicellular uncertainty set ψ on the basis of equation (3.10) to introduce the effect brought by the thermal nature of the room thermal dynamics, which leads to equation (3.11).

$$\begin{cases} \chi \dot{x} = D_{zd} \chi x + L_{zd} \chi u \\ y = Q\left(\chi x + x_0\right) \\ \left[D_{zd}\ L_{zd}\right] \in \psi_z \\ \left[D_{zd}\ L_{zd}\right] = \sum_{p=1}^{P} \left[D_{zp}\ L_{zp}\right] \\ \sum_{p=1}^{P} \phi_p = 1 \end{cases} \tag{3.11}$$

In equation (3.11), ψ_z is the multicellular uncertainty set and ϕ_p represents the non-negative constant. Since the indoor and outdoor thermal dynamic properties will change, the study specifies the bounds of convective heat transfer coefficient. This method can transform the original system into a convex multicellular model with 8 vertices, which can lead to a multicellular model of multi-zone HVAC room. Then the final model can be obtained after the discrete processing, as shown in equation (3.12).

$$\begin{cases} \chi x\left(k+1\right) = D_{zd} \chi x\left(k\right) + L_{zd} \chi u\left(k\right) \\ y = Q\left(\chi x\left(k\right) + x_0\right) \\ \left[D_{zd}\ L_{zd}\right] \in \psi_d \\ \left[D_{zd}\ L_{zd}\right] = \sum_{p=1}^{P} \left[D_{zp}\ L_{zp}\right] \\ \sum_{p=1}^{P} \phi_p = 1 \end{cases} \tag{3.12}$$

In equation (3.12), ψ_d is the new multi-cell uncertainty set. If the HVAC system matrix with more complex uncertainty parameters is considered, the number of multi-cell level vertices will cost expansion. The MPC algorithm can not solve it, but also lead to the failure of the system operation. So the study proposes the MPC-O algorithm, which applies N free control variables to the system at each initial control stage, and then uses a single state feedback control rate, as shown in equation (3.13).

$$\chi u\left(k+1\left|k\right.\right) = \begin{cases} \chi u\left(k\left|k\right.\right), t=0 \\ \chi u\left(k+1\left|k\right.\right), t=1 \\ \vdots \\ \varphi \chi u\left(k+1\left|k\right.\right), t \geq N \end{cases} \tag{3.13}$$

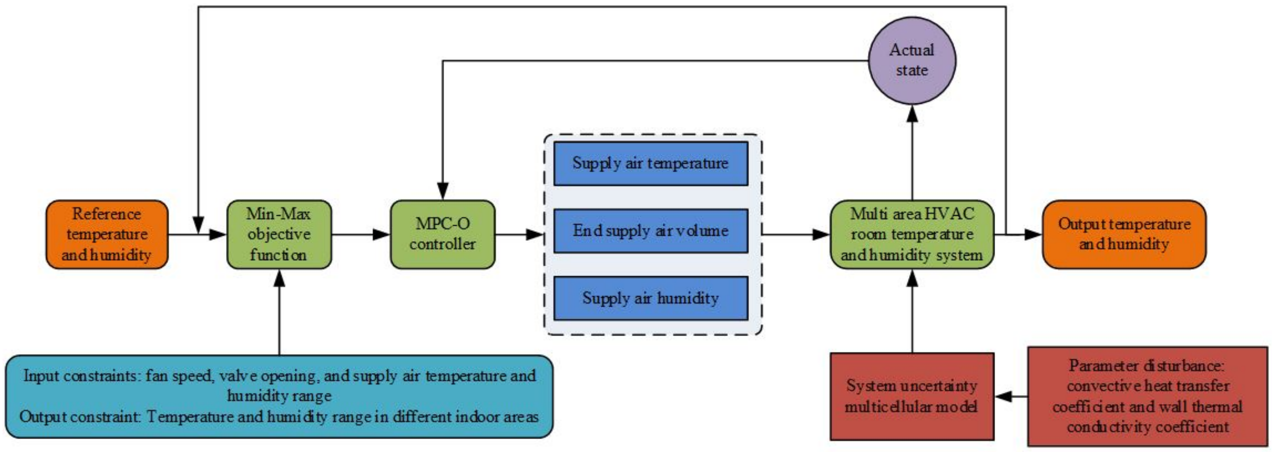

Fig. 3.4: Indoor comfort process improvement based on MPC-O strategy control

At this point, a new time-varying Lyapunov function is defined, as shown in equation (3.14).

$$V(t+1,k) - V(t,k) \leq -\left[\left\|\chi x(k+t\,|k)\right\|_{O_x}^2 + \left\|\chi u(k+t\,|k)\right\|_{R_x}^2\right] \tag{3.14}$$

Equation (3.15) can be obtained by adding up equation (3.13) from $t = M$ to ∞ and simplifying the right-hand term of the inequality with $-J_2(k)$.

$$-V(N,k) \leq -J_2(k) \tag{3.15}$$

At this point, the infinite time domain optimal problem is equivalent to minimizing the upper bound of $V(N,k)$, as shown in equation (3.16).

$$\max J_2(k) \leq \chi x(k+N)^T P(t,k)\,\chi x(k+N) \tag{3.16}$$

The transformation of the objective function from infinite time domain to finite time domain can be achieved through equation (3.16). The expression of the objective function for multi-zone HVAC room temperature and humidity optimization problem can be obtained in equation (3.17).

$$\min_{\eta_1,\eta_2,\chi U(k),\gamma(k),B_l} \left\|\chi x(k)\right\|_{O_x}^2 + \eta_1 + \eta_2 \tag{3.17}$$

In equation (3.17), both η_1 and η_2 are upper bounds. B_l denotes L symmetric positive definite matrices. Then LMI representation is applied to the upper bound, which is applied to the input-output constraints. Finally, the MPC-O algorithm is solved to obtain the state feedback control rate, and the calculation is shown in equation (3.18).

$$\begin{cases} \chi u(k+t\,|k) = \kappa \chi x(k+t\,|k) \\ \kappa = HG^{-1} \end{cases} \tag{3.18}$$

The synthesis of the above leads to an improved indoor comfort process based on the MPC-O strategy control, which is shown in Fig. 3.4.

In Fig. 3.4, it is necessary to multicellularize the perturbations that have in the modeling process. Meanwhile, the objective function related to temperature and humidity and air supply volume is established. The MPC-O algorithm is solved to obtain the optimal control volume under the constraints of the variable air volume HVAC system. Then the HVAC system is affected to obtain the actual output volume corresponding to

Table 4.1: Experimental parameter settings

Parameter	Numerical value	Parameter	Numerical value
$W_{a,A}$/(g/kg dry air)	18.3	$W_{a,C}$/(g/kg dry air)	18.5
$T_{a,A}$/C	28.0	$T_{a,C}$/C	29.6
$T_{iw,A}$/C	30.5	$T_{iw,C}$/C	30.8
$W_{a,B}$/(g/kg dry air)	18.5	$T_{ew,C}$/C	32.1
$T_{a,B}$/C	30.0	Prediction time domain and control time domain/min	30
$T_{iw,B}$/C	31.3	Sampling interval/min	5
The upper and lower limits of input constraints	[10, 10, 0.7, 20, 50], [-10, -10, -0.3, -10, -50]	Simulation duration	24
The upper and lower limits of output constraints	[32, 23.3, 34.6, 23.4, 35, 23.5], [23, 13.3, 24.6, 13.4, 25, 13.5]	Input rate of change constraint	[4, 3, 0, 5, 8, 10], [0, 0, 0, 0, 0, 0]

the different regions. Although the most important influencing factor in the indoor environment is the indoor temperature, a comprehensive evaluation cannot be made by considering only a single factor. Therefore, the study chooses the Predicted Mean Vote (PMV) index for evaluation, which integrates the key parameters such as temperature, humidity, average radiation, wind speed, etc. Meanwhile, PMV is an evaluation index that can accurately reflect the thermal comfort of the human body. The expression of PMV index used in the study is shown in equation (3.19).

$$PMV = 36.06W_i + 0.1403T_m + 0.1597T_i - 89.31 \tag{3.19}$$

In equation (3.19), W_i and T_i represent the temperature and humidity of the indoor environment. T_m represents the average radiant temperature. Although the room is divided into several zones, region C is the main activity area for human beings, so the study mainly analyzes region C to get the PMV index.

4. Analysis of MPC optimization algorithms and strategy results for HVAC systems. This study verified the performance and application effect of the MPC algorithm and its optimization algorithm. First, the study examined the performance of the multi-zone HVAC room comfort strategy control based on the MPC algorithm. Then the performance and application effect of the improved room comfort based on the MPC-O strategy control were analyzed.

4.1. Performance analysis of MPC-based multi-zone HVAC room comfort control. The study was simulated on the software MATLAB to verify the control performance of the multi-zone HVAC room comfort strategy based on the MPC algorithm. MATLAB mainly analyzes the temperature and humidity tracking of the different zones in the room under uncertain disturbance conditions. The study was conducted on a hot summer day in Wuxi and on the day with the highest temperature. The specific experimental parameters are set as in Table 1.

The experiments were conducted in a situation where only the comfort of a multi-zone HVAC room was considered (Environment 1), using the MPC algorithm and strategy to control the temperature and humidity in different zones of the room.

Fig. 4.1(a) to Fig. 4.1(c) show the comparison of temperature and humidity results of regions A, B, and C. In the presence of perturbation factors, the three regions responded quickly and reached the reference value, which took about 12 min. After reaching the reference set point, the temperature range of all the regions fluctuated around 0.35°C. The humidity was less affected by the perturbation factors and fluctuated only in a small range around 0.01g/kg dry air. 0.01g/kg dry air fluctuated in a small range. Since the above environment needed to keep the temperature and humidity stable throughout the day, which produced a great waste of power resources, the study introduced the price of electricity for simulation, i.e., Environment 2.

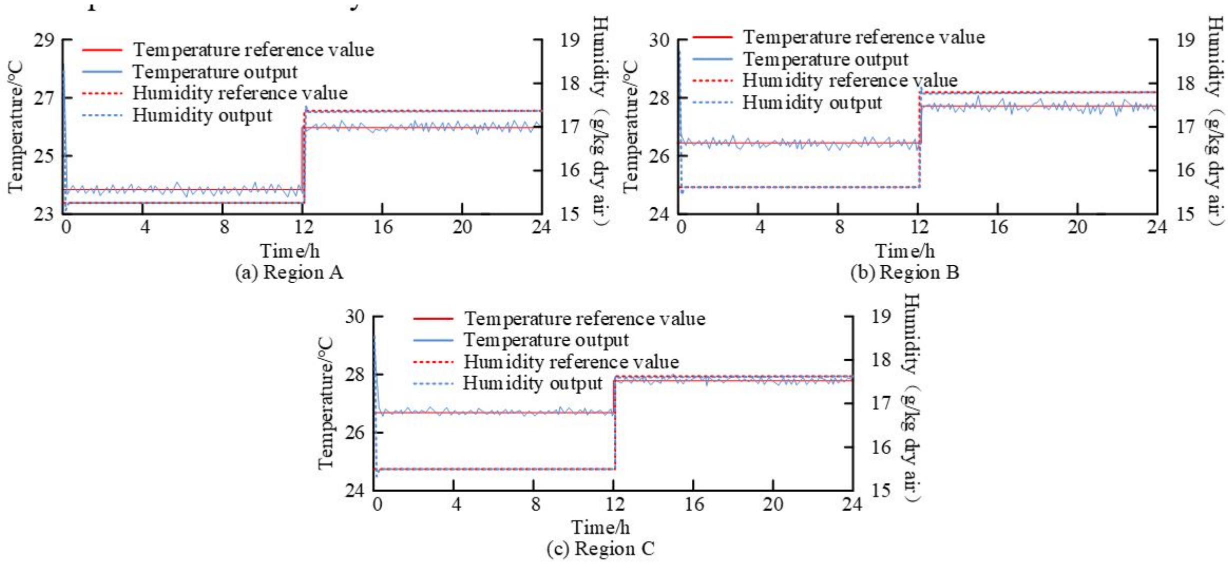

Fig. 4.1: Temperature and humidity results of different areas in multi-zone HVAC rooms based on MPC algorithm and strategy control

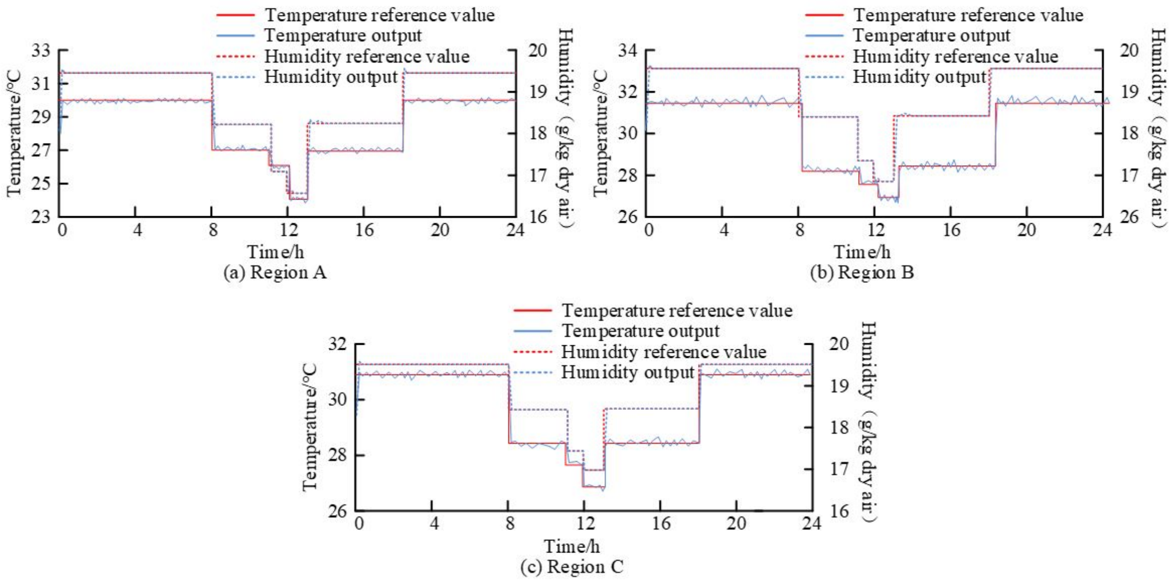

Fig. 4.2: Temperature and humidity control results of regions A, B, and C under Environment 2

Fig. 4.2(a) to Fig. 4.2(c) show the results of temperature and humidity control of areas A, B, and C under Environment 2, respectively. The different areas reached a stable state in 15 min. When the optimal temperature and humidity settings changed, the MPC algorithm also responded quickly. So the output results were consistent with the reference value, which indicated that the different areas were also better in terms of anti-interference in response to the changes in temperature and humidity. The study analyzed the fan speed, air flow rate, and cost of electricity in the two environments to further explore the changes in the two environments

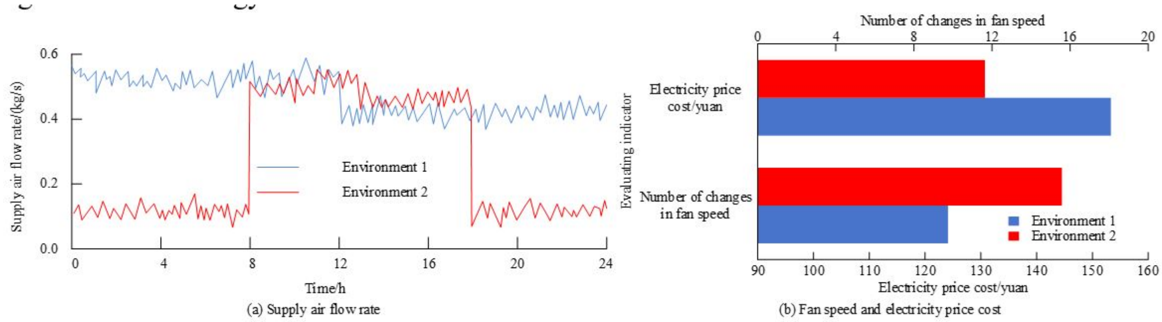

Fig. 4.3: Comparison results of supply air flow rate, fan speed, and electricity price cost based on MPC algorithm in two different environments

Table 4.2: Experimental parameter settings for Environment 3

Parameter	Numerical value	Parameter	Numerical value
$W_{a,A}$/(g/kg dry air)	18.3	$W_{a,C}$/(g/kg dry air)	18.5
$T_{a,A}$/C	26.6	$T_{a,C}$/C	30.7
$T_{iw,A}$/C	30.3	$T_{iw,C}$/C	31.6
$W_{a,B}$/(g/kg dry air)	18.5	$T_{ew,C}$/C	30.1
$T_{a,B}$/C	30.1	Sampling interval/min	6
$T_{iw,B}$/C	31.3	Simulation duration	6
The upper and lower limits of input constraints	[10, 10, 1, 10, 30], [-10, -10, -0.1, -10, -50]	The upper and lower limits of output constraints	[28, 21, 30, 23, 32, 23], [20, 15, 24, 16, 25, 14]
Output reference for the first 3 hours	[21.7, 15.8, 24.3, 16, 25.3, 16]	Output reference for the last 3 hours	[23.9, 17.3, 25, 17.5, 28, 17.2]

based on the MPC algorithm and strategy.

Fig. 4.3(a) and Fig. 4.3(b) show the results of MPC algorithm-based supply air flow rate, fan speed, and cost of electricity in two environments, respectively. If the temperature changed frequently, it greatly affected human comfort. But the results in case of Environment 2 saved 35.68% of the electricity cost while ensuring human comfort. In addition, the fans in Environment 1 changed only 10 times in the full control of the HVAC system, while it changed 16 times in Environment 2. In summary, the MPC algorithm was able to maintain a stable control effect in the presence of perturbing factors and still accomplished the initial energy saving goal in an environment where real-time tariffs were introduced. This method laid a solid foundation for the performance of subsequent MPC-O algorithms and strategies.

4.2. Analysis of results of improved indoor comfort based on MPC-O strategy control. The robustness of the MPC-O algorithm and the effect of different factors on indoor temperature and humidity control were examined in the study. The building envelope structure, indoor human activities and heat source changes, and the outdoor environment were denoted as factors X, Y, and Z. In addition, the study introduced the mainstream Robust Model Prediction (RMP) algorithm and MPC to conduct comparative experiments. In Environment 2, the study considered the impact of the three influencing factors. The above environment was set as Environment 3 to verify the superiority of the MPC-O algorithm and strategy. The experimental parameters at this time were set as in Table 4.2.

Experiments were conducted using the RMP algorithm with the MPC-O algorithm to analyze the effect of temperature and humidity control in different areas of the room under the conditions of Environment 3.

Fig. 4.4(a) to Fig. 4.4(c) show the results of temperature and humidity control corresponding to regions A, B, and C in Environment 3, respectively. The RMP algorithm was unable to fulfill the task of humidity control in HVAC rooms. When the HVAC system controlled by the algorithm was in operation, the humidity content

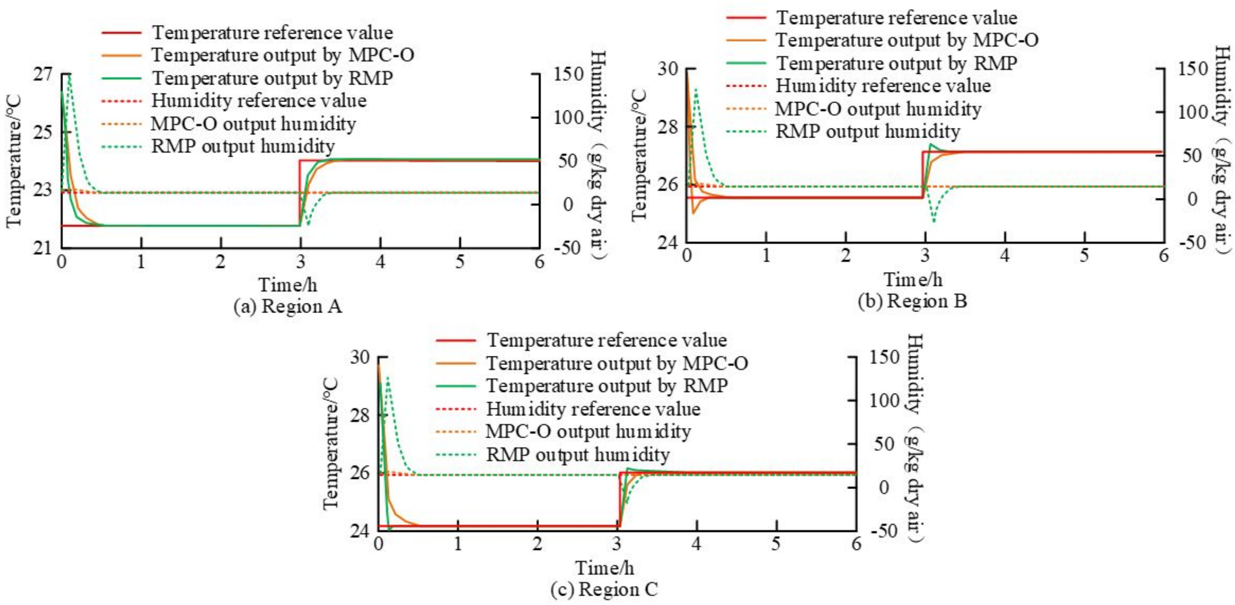

Fig. 4.4: BiLSTM neural network

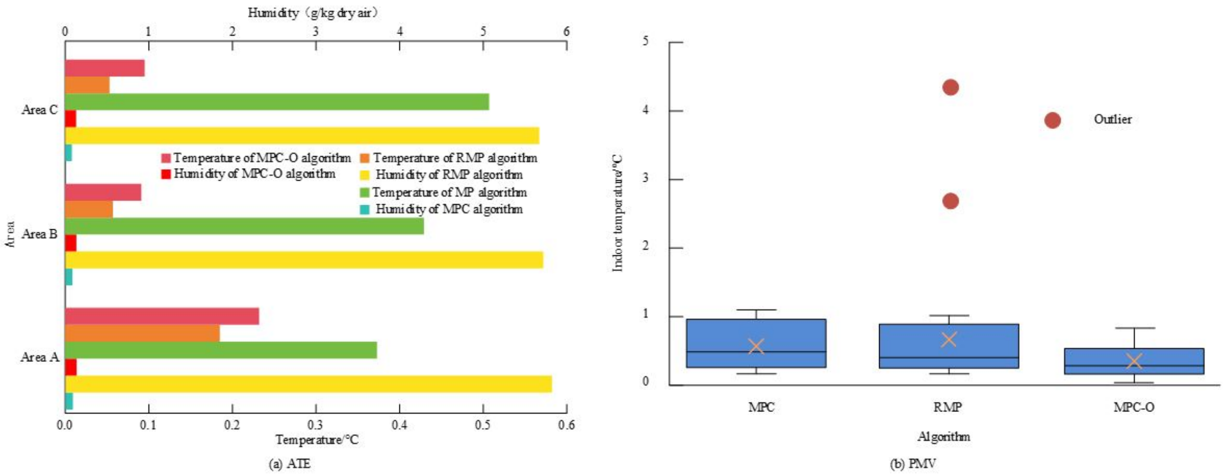

Fig. 4.5: Tracking and control effects under different algorithm controls

of the regions grew sharply to more than 100 g/kg dry air in 6 min, which was far beyond the actual control of the variable-air-volume HVAC system. This was far beyond the actual control range of the variable air volume HVAC system, leading to energy waste and environmental pollution and causing the system to malfunction. The MPC-O algorithm, on the other hand, showed a very small degree of overshooting in the initial state of each region, but it was quickly corrected after adjustment. So the temperature and humidity accurately tracked the reference value in most cases. The study used Average Tracking Error (ATE) and PMV for evaluation to more intuitively observe the tracking and control effects of different algorithms.

Fig. 4.5(a) and Fig. 4.5(b) show the ATE and PMV results under the control of different algorithms,

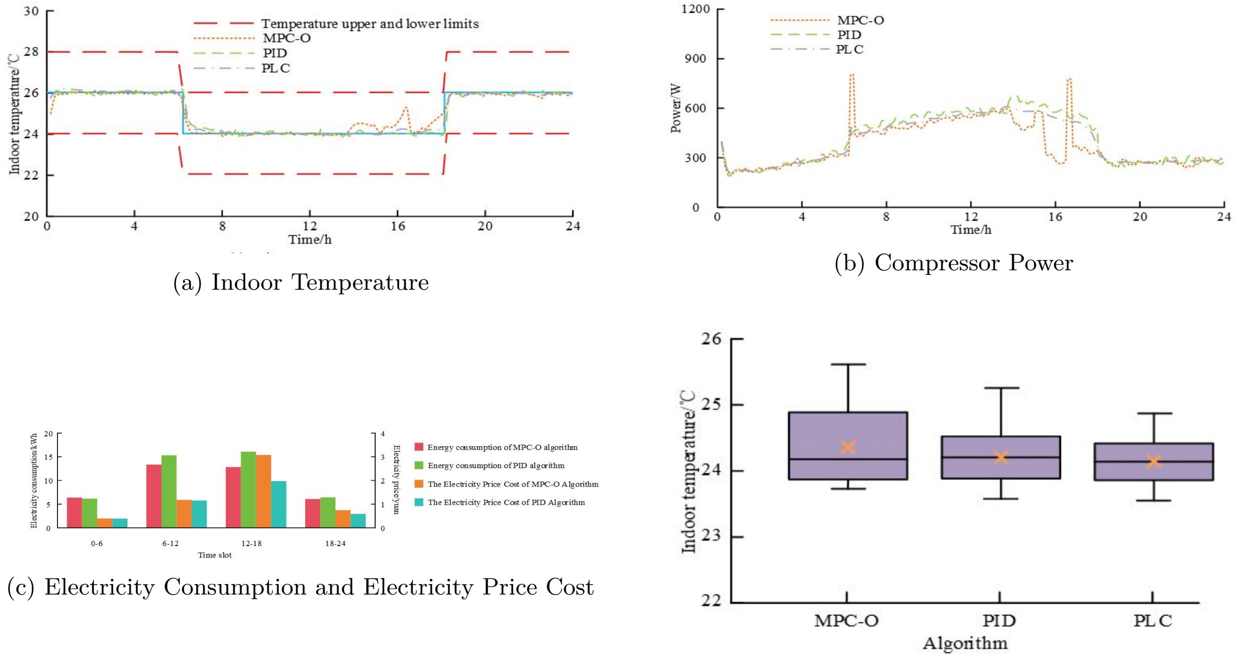

(a) Indoor Temperature

(b) Compressor Power

(c) Electricity Consumption and Electricity Price Cost

(d) Room Temperature Distribution

Fig. 4.6: The application effects of different algorithms in real scenarios

respectively. In each region, the ATE of the MPC algorithm was smaller, with an average of 0.082 g/kg dry air, but the temperature error was larger, with an average of 0.436°C. The difference in the ATE of the RMP algorithm for the humidity in different regions was very large, and the MPC-O algorithm had very good tracking effect of the temperature and humidity in all the regions. The ATE of MPC-O algorithm was 0.139℃ and 0.13g/kg dry air, respectively. In the PMV results, the average PMV of MPC, RMP, and MPC-O algorithms were 0.57, 0.63, and 0.32, respectively. In summary, the MPC-O algorithm had a better tracking and control effect. The study used traditional PID and PLC algorithms for comparison to further verify the energy-saving and comfort effect of MPC-O algorithm in practical applications. Experiments were carried out in the internal office of the building, with the total duration and sampling step set to 24h and 10min and set to 26℃, 24℃, and 26℃ at 0:00-6:00, 6:00-18:00, and 18:00-24:00, respectively.

The application effects of different algorithms in real scenarios are shown in Figure 10. Fig. 4.6 (a) to Fig. 4.6 (d) show the indoor temperature, compressor power, electricity consumption, electricity price cost, and room temperature distribution results under different algorithm controls. The proposed algorithm controlled the temperature to fluctuate around 0.1℃ around the reference value throughout the entire process, which increased the compressor power to 1200W in advance, quickly reaching the optimal temperature. During peak electricity consumption periods, it was quickly adjusted with minimal impact on comfort. The load demand was reduced during this period. In addition, the algorithm proposed in the study reduced total electricity consumption and electricity price costs by 12.11% and 22.54%, respectively, with an average indoor dimension of 24.5℃. The control of PID algorithm had hysteresis and poor energy-saving effect, with an average indoor temperature of 24.3℃. Moreover, the PID algorithm took some time for room temperature to reach a relatively stable state due to its limitations, making it impossible to predict the demand for future increases in indoor cooling load. In addition, different algorithms did not have significant energy-saving effects during periods of low electricity prices. The advantages of the proposed algorithm were only demonstrated during peak electricity consumption periods. It not only significantly reduced energy efficiency and costs, but also alleviated the pressure on the power grid. The average indoor temperature of the PLC algorithm was 24.6℃, which had a poor effect on maintaining indoor comfort. In summary, the proposed algorithm achieved energy conservation and effectively promoted the sustainable development of electricity during peak hours of practical application compared with the application effect of traditional algorithms, while ensuring indoor comfort.

5. Conclusion. The HVAC system is an air conditioner integrating ventilation, heating and air conditioning. However, with the development of urban intelligence, its comfort and energy saving face great challenges. First, the study designed the MPC algorithm and strategy for control to improve the intelligent development of HVAC system, energy saving and human comfort. Then an MPC-O algorithm was proposed based on LMI inequality for the external uncertainty perturbation. The experimental results showed that the humidity content of the RMP algorithm control of each region grew sharply to more than 100g/kg dry air in 6min under the influence of different factors. The MPC-O algorithm of each region in the initial state had little overshooting. After adjustment, this algorithm got quickly corrected. In addition, the RMP algorithm of different regions of humidity ATE difference was very large, while the MPC-O algorithm in the various regions of the temperature and humidity ATE were 0.139℃ and 0.13g/kg dry air. The average PMV of MPC, RMP, and MPC-O was 0.57, 0.63, and 0.32, respectively. In the practical application, the MPC-O algorithm made the temperature in the whole controlling in the 0.1°C fluctuation around the reference value. The total power consumption and electricity cost were reduced by 12.11% and 22.54%, respectively, with an average indoor dimension of 24.5°C. The average indoor temperature of the PID algorithm was at 24.3°C. In summary, the method proposed by the study has better performance and can balance comfort and energy saving in practical applications. However, there are still shortcomings in the study, which enhances indoor comfort by adjusting the air flow supplied from the outlet. But in the actual duct delivery, there are losses caused by other factors such as wind force and moisture content. So other factors can be considered to construct the model in future research.

REFERENCES

[1] Binqing, C., Yujing, H. & Xinhuan, H. Analysis of Green Building Supply Under Compound Environmental Regulation by Evolutionary Game. *Journal Of Systems Science & Complexity.* **42**, 3339-3354 (2022)

[2] Koranteng, C., Simons, B., Gyimah, K. & Nkrumah, J. Ghana's Green Building Assessment Journey: An Appraisal of the Thermal Performance of an Office Building in Accra. *Journal Of Engineering, Design And Technology.* **21**, 188-205 (2023)

[3] Teng, J., Yin, H. & Wang, P. Study on the Operation Strategies and Carbon Emission of Heating Systems in the Context of Building Energy Conservation. *Energy Science And Engineering.* **11**, 2421-2430 (2023)

[4] Wheeler, V., Kim, J., Daligault, T., Rosales, B., Engtrakul, C., Tenent, R. & Wheeler, L. Photovoltaic Windows Cut Energy Use and CO2 Emissions by 40% in Highly Glazed Buildings. *One Earth.* **5**, 1271-1285 (2022)

[5] Garay, A., Ruiz, A. & Guevara, J. Dynamic Evaluation of Thermal Comfort Scenarios in a Colombian Large-scale Social Housing Project. *Engineering Construction & Architectural Management.* **29**, 1909-1930 (2022)

[6] Hebbi, C. & Mamatha, H. Comprehensive Dataset Building and Recognition of Isolated Handwritten Kannada Characters Using Machine Learning Models. *Artificial Intelligence And Applications.* **1**, 179-190 (2023)

[7] Saminu, S., Xu, G., Zhang, S., Kader, I., Aliyu, H., Jabire, A., Ahmed, Y. & Adamu, M. Applications of Artificial Intelligence in Automatic Detection of Epileptic Seizures Using EEG Signals: A Review. *Artificial Intelligence And Applications.* **1**, 11-25 (2023)

[8] Li, Y. Study on Load Estimation Method of HVAC System in Large Public Gymnasium. *International Journal Of Global Energy Issues.* **45**, 14-25 (2023)

[9] Satar, M., Mazlan, A., Hamdan, M., Isa, M. & Ghaper, M. Validation of Clicking-type Noise and Vibration in Automotive HVAC System. *International Journal Of Automotive And Mechanical Engineering.* **18**, 8489-8497 (2021)

[10] Jani, D. A Recent Development in Desiccant Assisted HVAC System. *ASHRAE Journal.* **24**, 26-52 (2021)

[11] Vogt, M., Koch, K., Turetskyy, A., Cerdas, F., Thiede, S. & Herrmann, C. Model-based Energy Analysis of a Dry Room HVAC System in Battery Cell Production. *Procedia CIRP.* **98** pp. 157-162 (2021)

[12] Wang, Z., Gao, F., Zhao, Y., Yin, Y. & Wang, L. Improved A* Algorithm and Model Predictive Control-Based Path Planning and Tracking Framework for Hexapod Robots. *Industrial Robot.* **50**, 135-144 (2023)

[13] Ren, J., Wang, Z. & Fang, F. Model Predictive Control Based Defensive Guidance Law in Three-Body Engagement. (2022)

[14] He, N., Xu, Z. & Shen, C. An Error Gradient and Accumulation-type Event-driven Model Predictive Control with Relative Thresholds for Perturbed Nonlinear Systems. *IET Control Theory & Applications.* **16**, 1873-1863 (2022)

[15] Wang, S., Li, J., Hou, Z., Meng, Q. & Li, M. Composite Model-free Adaptive Predictive Control for Wind Power Generation Based on Full Wind Speed. *CSEE Journal Of Power And Energy Systems.* **8**, 1659-1669 (2022)

[16] Ile, A., Matuko, J. & Lazar, M. Piece-wise Ellipsoidal Set-based Model Predictive Control of Linear Parameter Varying Systems with Application to a Tower Crane. *Asian Journal Of Control.* **23**, 1324-1339 (2021)

[17] Zamani, M., Rahmani, Z. & Rezaie, B. A Novel Framework of Model Predictive Control for Controlling a Class of Nonlinear System in the Presence of Uncertainty. *Journal Of Vibration And Control.* **28**, 1279-1294 (2022)
[18] Rakovi, S., Zhang, S., Dai, L., Hao, Y. & Xia, Y. Convex Model Predictive Control for Collision Avoidance. *IET Control Theory And Applications.* **15**, 1270-1285 (2021)
[19] Decardi-Nelson, B. & Liu, J. Robust Economic Model Predictive Control with Zone Control. *IFAC-PapersOnLine.* **54**, 237-242 (2021)
[20] Sun, H., Zou, T., Liu, J. & Wang, M. Double-layer Model Predictive Control Integrated with Zone Control. *ISA Transactions.* **114**, 206-216 (2021)

Edited by: Zhengyi Chai
Special issue on: Data-Driven Optimization Algorithms for Sustainable and Smart City
Received: Feb 27, 2024
Accepted: May 6, 2024